Electronic Supplementary Material (ESI) for ChemComm.
This journal is © The Royal Society of Chemistry 2015

SUPPORTING INFORMATION ACCOMPANYING:

Ground to Conduct: Mechanochemical Synthesis of a Metal-Organic Framework with High Proton Conductivity

Dariusz Matoga, Marcin Oszajca, Marcin Molenda

Contents:

Synthetic procedures

All chemicals and solvents (of analytical grade) were purchased from commercial sources (Aldrich, POCh, Polmos) and were used as supplied unless otherwise stated. Ethanol (Polmos) contained water 8% by volume. $\{[Mn_2(ina)_4(H_2O)_2]\cdot 2EtOH\}_n$ (JUK-1) was synthesized according to the literature method.[S1]

Compound $\{(NH_4)_2[Mn(ina)_2(NCS)_2]\}_n\cdot xH_2O$ (JUK-2)

JUK-1 (80.0 mg; 0.220 mmol) and NH_4SCN (33.5 mg; 0.440 mmol) were ground in an agate mortar in air at room temperature for approx. 10 min. Within this time approx. 100-120 μL 92% EtOH was added twice (liquid-assisted grinding, LAG) and evaporated. Pale-yellow powder of JUK-2 was obtained (99.4 mg, 0.220 mmol) was obtained. Yield: 100%. Anal. Found: C, 36.89; H, 3.51; N, 18.46; S, 14.29. Calcd for $C_{14}H_{16}N_6O_4S_2Mn$ (anhydrous JUK-2): C, 37.25; H, 3.57; N, 18.62; S, 14.21%. Calcd for $C_{14}H_{16.5}N_6O_{4.25}S_2Mn$ ($\{(NH_4)_2[Mn(ina)_2(NCS)_2]\}_n\cdot 0.25H_2O$): C, 36.88; H, 3.65; N, 18.43; S, 14.07%. IR (ATR, cm^{-1}): $\nu(COO_{as})$ 1580vs**,** $\nu(COO_s)$ 1408s, $\nu(CN)_{SCN}$ 2103vs, $\nu(NH)_{ammonium}$ 3236m 3186m. UV-vis (solid state) λ, nm: 310sh, 266, 232, 215.

Neat grinding: It has been confirmed by IR spectroscopy and PXRD that already after 1 min of neat grinding (NG), JUK-2 is quantitatively formed (Fig. S1 below).

Compound $[Mn(NCS)_2(py)_4]$

JUK-1 (15.0 mg; 0.0413 mmol) was added to pyridine (2 mL) and sonicated approx. 2-5 min. until dissolution. Then the solution of NH_4SCN (6.3 mg, 0.0826 mmol) dissolved in pyridine (1 mL) was added. After two week colorless crystals of $[Mn(py)_4(NCS)_2]$ were filtered and dried in air. Yield: (19.1 mg; 95%). Anal. Calcd for $C_{22}H_{20}MnN_6S_2$: C, 54.20; H, 4.14; N, 17.24. Found: C, 53.70; H, 4.05; N, 17.11%. IR (ATR, cm^{-1}): ν(SCN) 2058vs.

The same compound was obtained when 15.7 mg or 62.9 mg (5-fold or 20-fold excess over Mn, respectively) of NH_4SCN was used instead of 6.3 g.

Note: In one of the trials, with an addition of approx. 20-fold excess of solid NH_4SCN, the formation of yellow crystals of $(pyH)_3[Mn(NCS)_5]$ has been observed. The crystals have been filtered and dried in air. IR (ATR, cm^{-1}): ν(SCN) 2050vs, ν(NH) 3219m, 3161m, 3126w. The identity of the compound has been verified by SC-XRD (see below).

Efficacy of grinding of JUK-1 with NH_4SCN in the conversion of JUK-1 to JUK-2 (Fig. S2):

Experimental details (sample preparations related to curves from Fig. S2) and comments.

JUK-1 and NH_4SCN were ground separately prior to experiments. In each experiment they were weighed to satisfy the 1:2 molar ratio. Bottom to top:

i) EtOH (1.0 mL) was added to JUK-1 (15.5 mg) and NH_4SCN (6.5 mg) and the mixture was left for approx. 20h at room temperature (without grinding). After that, solid sample was filtered off and dried in air. The IR spectrum is identical to that of JUK-1.

ii) EtOH (50 μL; the amount corresponding to LAG conditions) was added to JUK-1 (16.7 mg) and NH_4SCN (7.0 mg) and the mixture was left (without grinding) at room temperature until ethanol was evaporated. The IR spectrum of the sample indicates the presence of unreacted NH_4SCN (pronounced signal at 2067 cm^{-1} is observed).

iii) JUK-1 (15.0 mg) and NH_4SCN (6.3 mg) were ground at room temperature for approx. 2 minutes. The IR spectrum indicates the presence of JUK-2 which was additionally confirmed for the analogous sample obtained after shorter grinding time (1 min) by the PXRD pattern in Fig. S1).

All above experiments indicate the efficacy of grinding in the conversion of JUK-1 to JUK-2.

Control experiments to test the possibility of formation of JUK-2 under various conditions in solution (Figs. S3 and S4)

Several trials described below have been carried out with various manganese(II) salts, isonicotinic acid and ammonium thiocyanate. In all experiments a manganese(II) salt (0.250 mmol), isonicotinic acid (61.6 mg; 0.500 mmol) and NH_4SCN (38.1 mg; 0.500 mmol) was mixed with a solvent (10.0 mL) and heated in closed vials at 70°C (EtOH) or at 130 °C (DMF) for approx. 72h.

i) $Mn(NO_3)_2 \cdot 4H_2O$ (62.8 mg); ethanol: white precipitate MnNO_etoh
ii) $MnCl_2$ (31.5 mg); ethanol: white precipitate MnCL_etoh
iii) $Mn(O_2CCH_3)_2 \cdot 4H_2O$ (61.3 mg); ethanol: white precipitate MnAC_etoh
iv) $Mn(NO_3)_2 \cdot 4H_2O$ (62.8 mg); dmf: white precipitate MnNO_dmf
v) $MnCl_2$ (31.5 mg); dmf: no precipitate
vi) $Mn(O_2CCH_3)_2 \cdot 4H_2O$ (61.3 mg); dmf: white precipitate MnAC_dmf

Note: Analogous additional control experiments have been performed in dmf at 70°C and a precipitate was only observed when the starting salt was $Mn(O_2CCH_3)_2 \cdot 4H_2O$. The IR spectrum of this product was identical with that of MnAC_dmf (after reaction at 130 °C).

All obtained solids have been screened with IR spectroscopy (Figs. S3 and S4 below). In all of the trials JUK-2 was not formed; no characteristic *ν*(CN) band of the SCN group was observed for obtained solids. Sample MnAC_etoh was identified as JUK-1.

Grinding of JUK-1 with ionic substances different from NH_4SCN (LiSCN, KSCN, NH_4Br and NH_4Cl) (IR spectra: Figs. S5-S8)

JUK-1 (15.0 mg; 0.0413 mmol) and KSCN (8.0 mg; 0.083 mmol) were ground in an agate mortar in air at room temperature for approx. 10 min. Within this time approx. 20 μL 92% EtOH was added twice (liquid-assisted grinding, LAG) and evaporated. Pale-yellow powder of the resulting solid was subject to IR measurements (see below).
Analogous grinding was performed for JUK-1 (15.0 mg; 0.0413 mmol) and LiSCN or NH_4Cl or NH_4Br (each with the amount of 0.083 mmol). Grinding with thiocyanates of alkali metals gave pastes whereas grinding with ammonium salts gave powders.

Elemental analysis for JUK-2 conditioned at 35°C, 80%RH for 94 hours, then dried in a vacuum dryer at 70 °C, 50 mbar for 2 hours (PXRD pattern: Fig. S23)

Found: C, 38.29; H, 2.98; N, 15.06; S, 14.08%. Calcd for $C_{14}H_{15}N_5O_5S_2Mn$ ($\{(NH_4)(H_3O)[Mn(ina)_2(NCS)_2]\}_n$): C, 37.17; H, 3.34; N, 15.48; S, 14.18%.

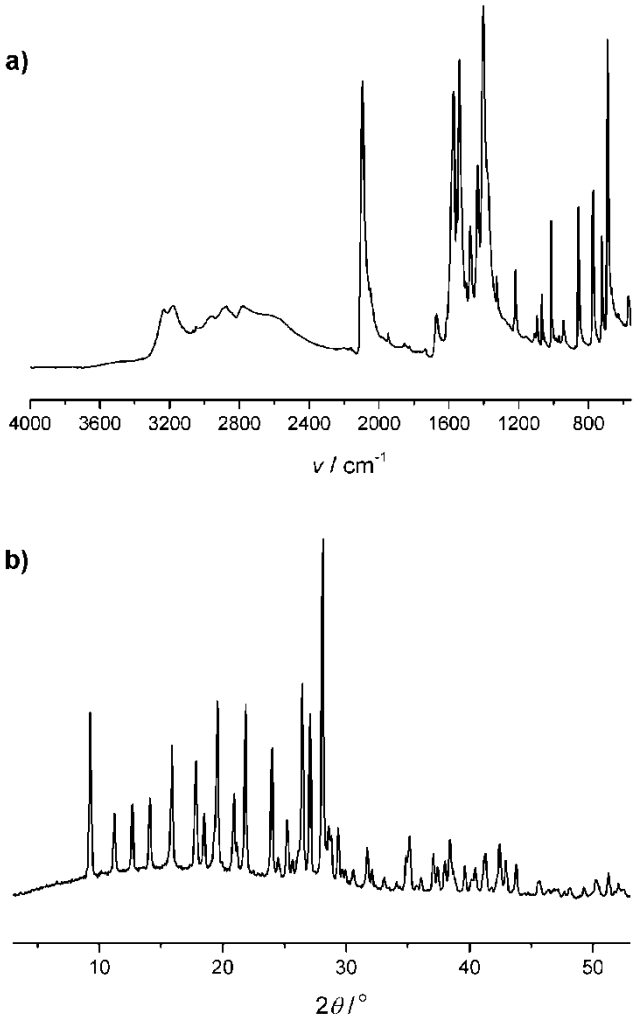

Figure S1. IR spectrum (a) and PXRD pattern (b) recorded for the sample after 1 min neat grinding of JUK-1 and NH_4 SCN.

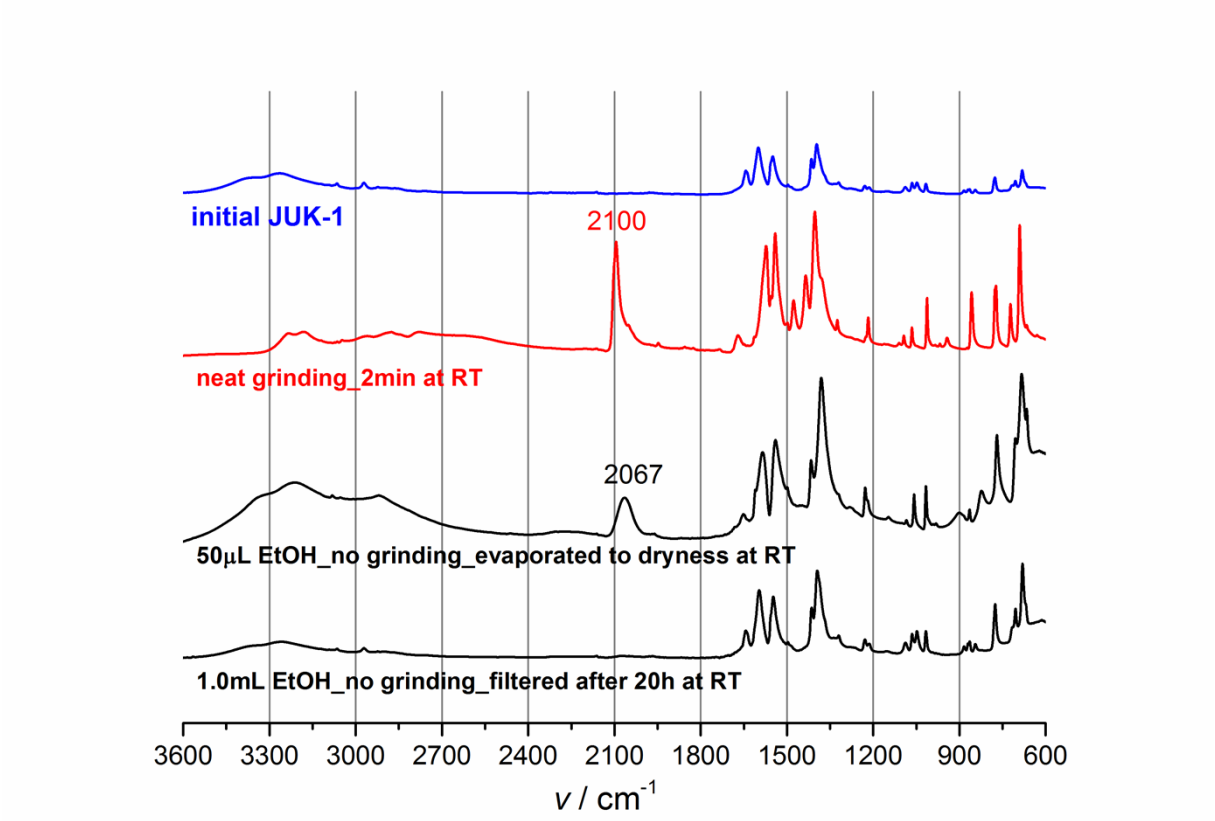

Figure S2. IR spectra of JUK-1 and NH_4SCN mixtures (1:2 molar ratio) after neat grinding (red curve) and after adding EtOH without grinding (black curves). The IR spectrum of initial JUK-1 is given for comparison (blue curve). RT - room temperature.

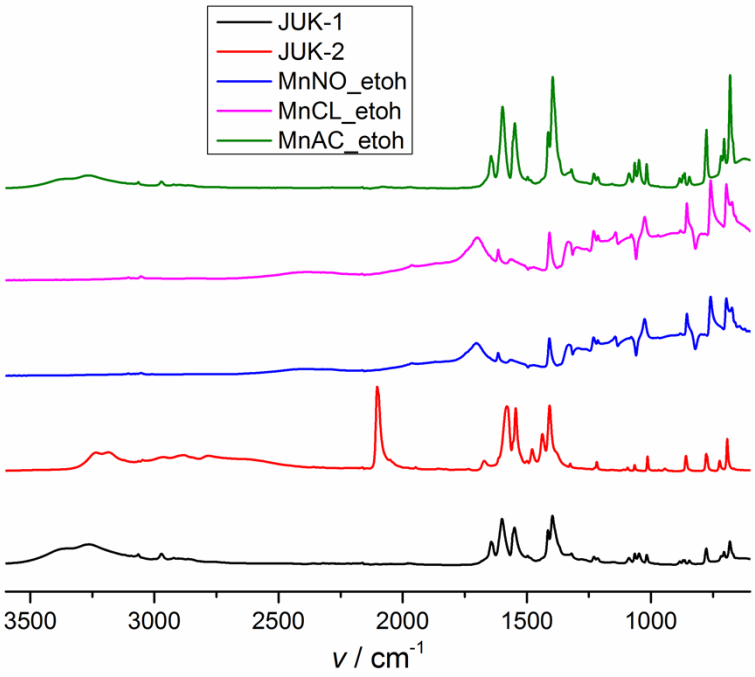

Figure S3. IR spectra of samples obtained in control experiments in ethanol starting from various manganese(II) salts, isonicotinic acid and NH_4SCN. The IR spectrum of initial JUK-1 and JUK-2 are given for comparison.

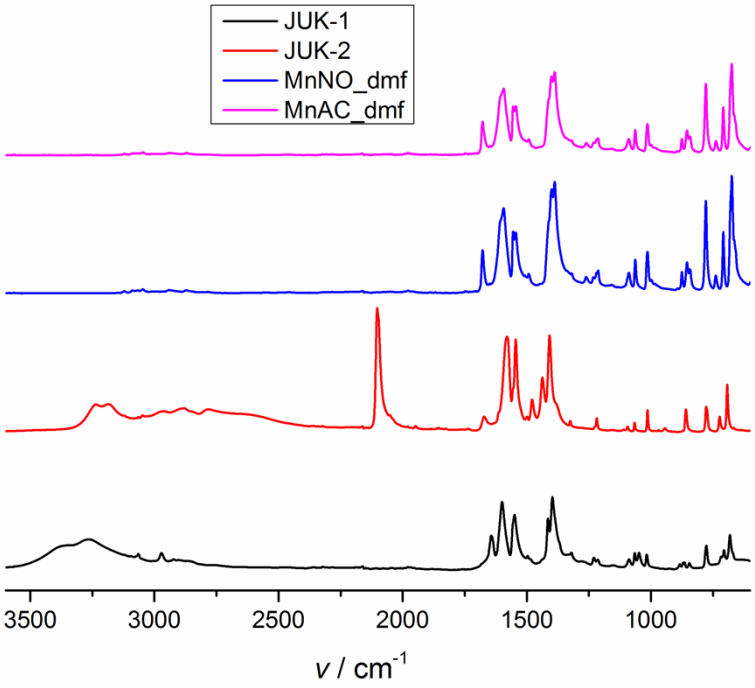

Figure S4. IR spectra of samples obtained in control experiments in dmf starting from various manganese(II) salts, isonicotinic acid and NH_4SCN. The IR spectrum of initial JUK-1 and JUK-2 are given for comparison.

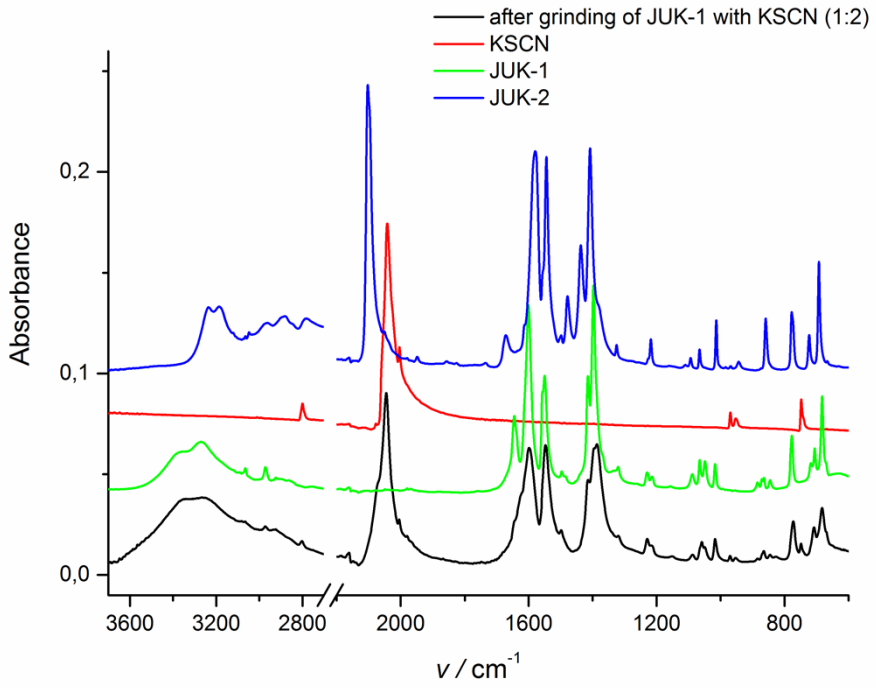

Figure S5. IR spectra recorded after grinding of JUK-1 and KSCN (1:2 molar ratio). IR spectra of JUK-1, KSCN and JUK-2 are given for comparison.

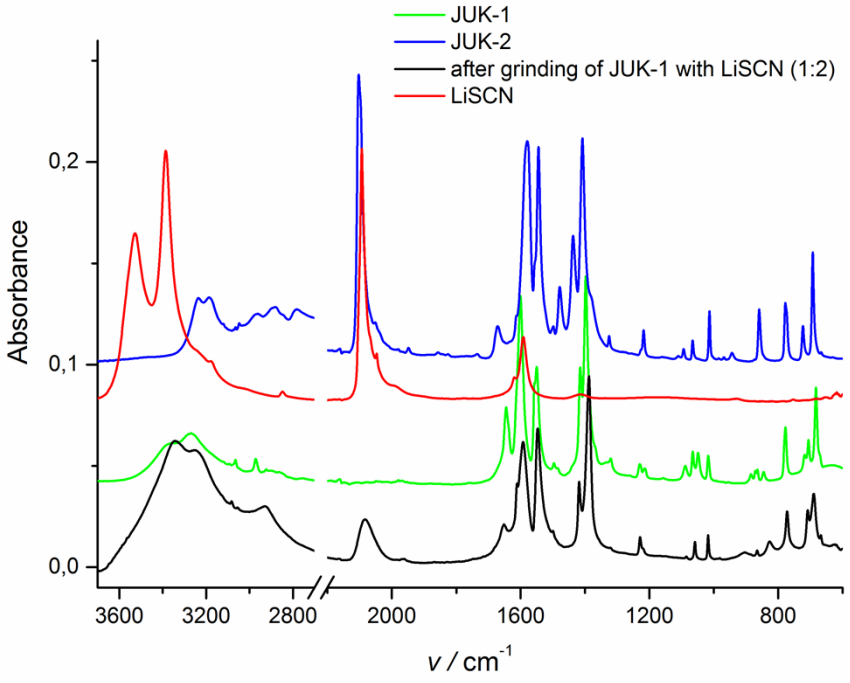

Figure S6. IR spectra recorded after grinding of JUK-1 and LiSCN (1:2 molar ratio). IR spectra of JUK-1, LiSCN and JUK-2 are given for comparison.

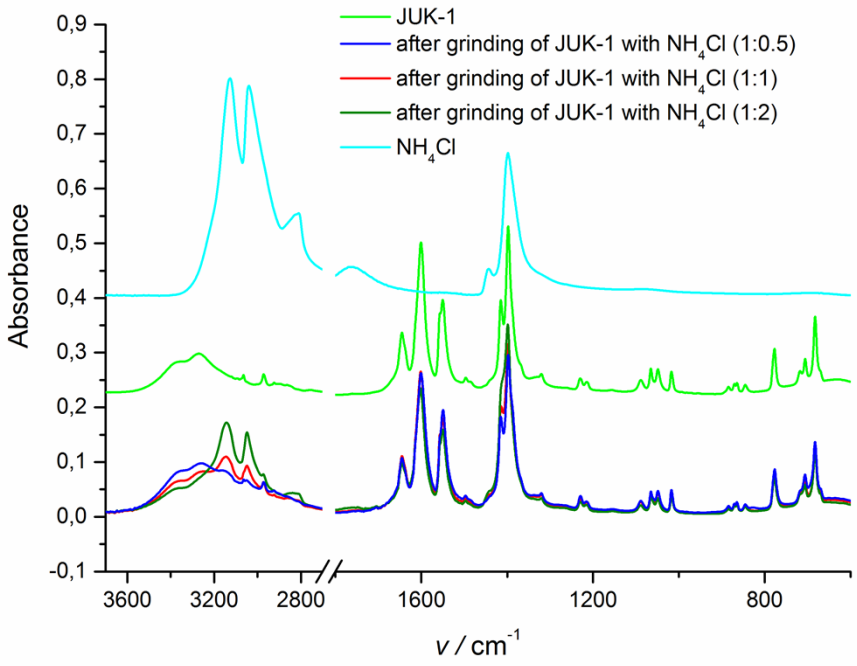

Figure S7. IR spectra recorded after grinding of JUK-1 and NH_4Cl (1:0.5, 1:1 and 1:2 molar ratios). IR spectra of JUK-1 and NH_4Cl are given for comparison.

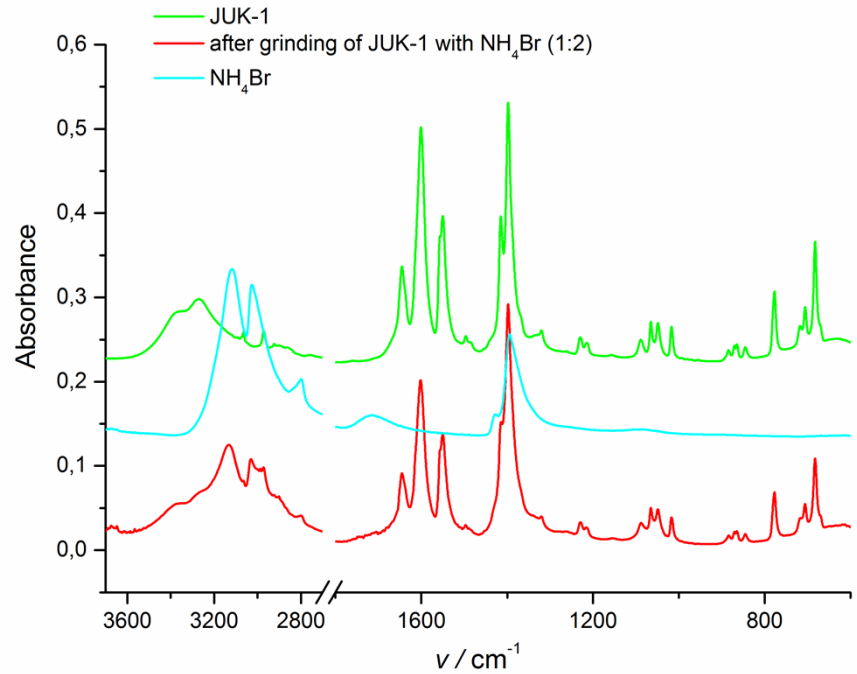

Figure S8. IR spectra recorded after grinding of JUK-1 and NH_4Br (1:2 molar ratio). IR spectra of JUK-1 and NH_4Br are given for comparison.

PXRD data collection and structure refinement details for $\{(NH_4)_2[Mn(ina)_2(NCS)_2]\}_n \cdot xH_2O$ (JUK-2)

Powder X-ray diffraction (PXRD) measurement was performed with PANalytical X'Pert PRO MPD system equipped with a Cu-tube (working parameters of 40kV and 30mA) and position sensitive PIXCEL detector with a graphite diffracted beam monochromator. Ground powder was packed inside a borosilicate glass capillary (0.5 mm diameter manufactured by Hilgenberg GmbH) and mounted on a standard goniometer head attached to a capillary spinner. Elliptical multilayer X-ray focusing mirror was applied to obtain a high intensity beam with good resolution. The measurement was performed in a multiple-scan experiment (4 scans) with each point of the diffraction pattern collected for ca. 800s (ca. 170 min/scan) in the range of 3-85° (2θ). The collected data was checked for any changes between individual scans and then all of them were summed and binned to 0.02° 2θ step.

The obtained data was indexed using N-Treor[S3] procedure implemented in EXPO 2013[S4] and the calculated cell parameters are reported in Table X. Volume of this cell is consistent with predictions based on the results of elemental analysis. Using systematic absences extinction symbol was identified and space group $P2_1/c$ was selected for the structure solution attempts. Application of direct methods was at most only partially successful as in some obtained models Mn atoms as well as SCN groups were reasonably located. Due to this global optimization techniques were utilized using parallel tempering algorithm implemented in FOX[S5]. Mn atom, SCN^- anion, isonicotinate anion and nitrogen atom (representing an ammonium cation) were used as components for model optimization procedure. As a result of optimization calculations with rigid molecule models reasonable structural descriptions were obtained giving a flat-square coordination of nitrogen atoms from nicotinic acid and SCN groups. Since positions of the isonicotinate anion allowed for oxygen atoms to function as ligands in the coordination sphere of Mn, further calculations were performed with an additional parameter describing the rotation of carboxylic group in relation to the aromatic ring plane. The resulting structure with an octahedral coordination around Mn atoms was introduced to Jana2006[S6] to perform structure refinement using Rietveld method.[S7] To make the refinement more stable Levenberg-Marquardt algorithm was applied (approach to improve the non-linear least squares procedure) with a fudge factor of 0.01. To properly model the electron density of the ammonium cations occupancy of the respective nitrogen atom in the structure was changed to 1.43 to take into account the contribution of hydrogen atoms. This approach was taken since there was no possible way to unambiguously determine the orientation of the molecule (select hydrogen atoms positions). Calculated diffraction pattern based on the final structure model shows good agreement with the one measured for the studied sample. The quality of the fit is reflected in the R-factors values (presented in Table S1) and shape of the difference curves (Figure S9).

During structure analysis two impurity lines were identified (indicated with black squares in Figure S9). Parallel to further attempts at structure solution in the obtained cell its supercells were also tested for possible structure models. Structure solutions performed in supercells did not give any satisfactory models so the original cell was considered as the proper one and additional peaks in the diffraction pattern were assigned to unknown impurity/ies as no reasonable assignment of crystalline phase (neither substrate nor other substance) could be given with the use of PDF-4+ database.

Crystallographic information file (CIF) has been deposited with the Cambridge Crystallographic Data Centre (CCDC): CCDC-1003007. Copy of the data can be obtained free of charge via http://www.ccdc.cam.ac.uk/conts/retrieving.html, or from the Cambridge Crystallographic Data Centre, 12 Union Road, Cambridge CB2 1EZ, UK; fax: +44 1223 336 033; or e-mail: deposit@ccdc.cam.ac.uk.

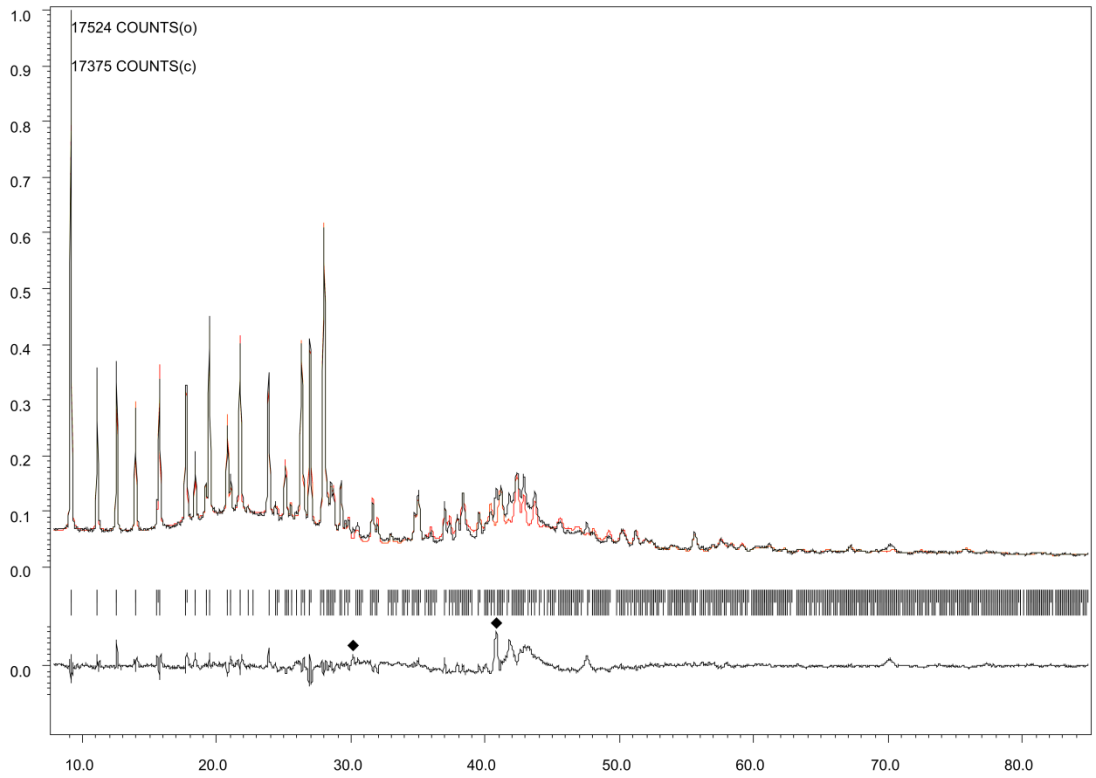

Figure S9. The observed (black line) and calculated (red line) PXRD patterns of JUK-2 along with the difference curve (bottom black line). two detected impurity lines are highlighted (black squares).

Table S1. Data collection and structure refinement details for $\{(NH_4)_2[Mn(ina)_2(NCS)_2]\}_n \cdot xH_2O$ (JUK-2).

	JUK-2
empirical formula	$C_{14}H_{16}MnN_6O_4S_2$
formula weight	451.4
crystal system	monoclinic
space group	P $2_1/c$
a (Å)	9.723(3)
b (Å)	14.061(4)
c (Å)	7.1516(18)
α (deg)	90
β (deg)	97.92(3)
γ (deg)	90
V (Å^3)	968.4(5)
Z	2
T (K)	293
D_c (Mg/m^3)	1.5475
μ (mm^{-1})	7.861
$2\theta_{min}/2\theta_{max}/2\theta_{step}$ (°)	7.02/84.98/0.02
R_p	0.0645
R_{wp}	0.0921
wR	0.1131

Table S2. Selected bond lengths (Å) and angles (°) for $\{(NH_4)_2[Mn(ina)_2(NCS)_2]\}_n \cdot xH_2O$ (JUK-2).

Bond lengths	
Mn–X	
Mn1–N13	2.22(11)
Mn1–N7	2.29(4)
Mn1–O1	2.29(9)
S–C	
S11–C12	1.66(10)
C–N	
C12–N13	1.13(13)
C–O (carboxylate)	
C2 –O1	1.24(15)
C2 –O3	1.25(15)
Bond angles	
N–Mn–N	
N13–Mn1–N13’	180.0(5)
N7–Mn1–N7’	180.0(5)
N13–Mn1–N7’	88(3)
N13–Mn1–N7	92(2)
O–Mn–O	
O1–Mn1–O1’	180.0(5)
N–C–S	
N13–C12–S11	179(9)
C–N–Mn	
C12–N13–Mn1	168(10)
O–Mn–N	
O1–Mn1–N7	88(3)
O1–Mn1–N7’	92(2)
O1–Mn1–N13’	95(4)
O1–Mn1–N13	85(4)

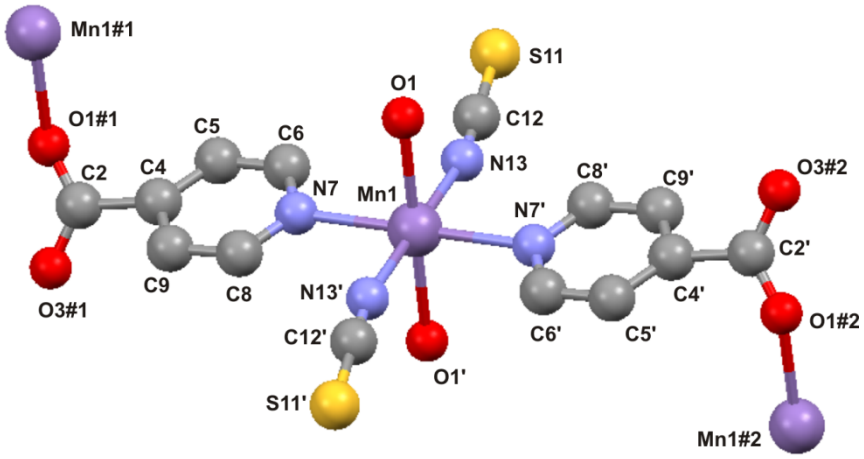

Figure S10. Partial view of the X-ray crystal structure of the anionic framework in $\{(NH_4)_2[Mn(ina)_2(NCS)_2]\}_n \cdot xH_2O$ (JUK-2) with atom labeling scheme.

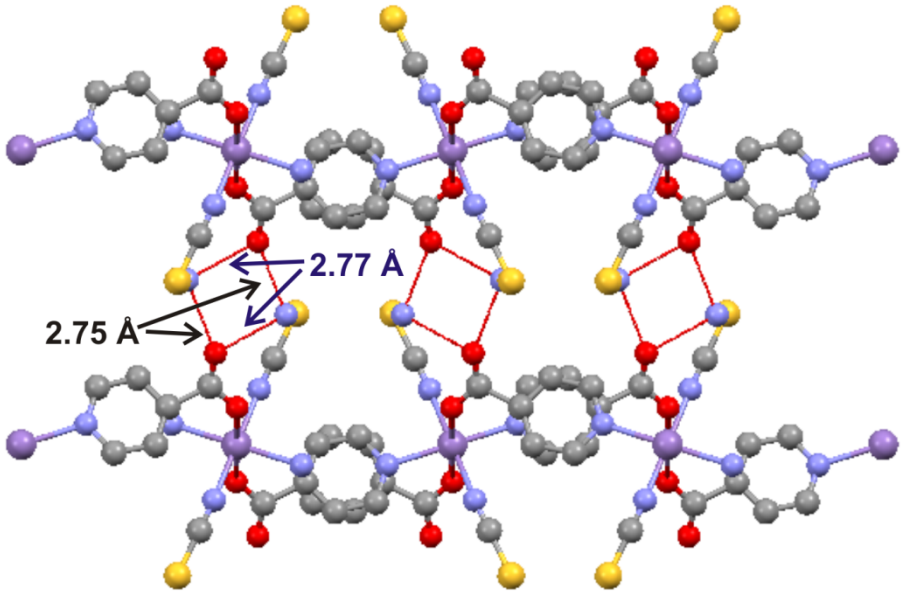

Figure S11. Interlayer N–H···O hydrogen bonds, shown as red lines, in $\{(NH_4)_2[Mn(ina)_2(NCS)_2]\}_n \cdot xH_2O$ (JUK-2) viewed along the *c* axis (H atoms omitted, Mn – purple, O – red, N Or NH_4^+ group – blue, S – yellow, C – grey).

SC-XRD data collection and structure refinement details for $(pyH)_3[Mn(NCS)_5]$

The crystals of $(pyH)_3[Mn(NCS)_5]$ suitable for X-ray analysis were selected from the material prepared as described under Synthetic procedures. Intensity data were collected on Oxford Diffraction SuperNova dual source diffractometer with an Atlas electronic CCD area detector using Mova microfocus Cu-Kα radiation source (λ =1.5418 Å) and graphite monochromator. Cell refinement and data reduction was performed using firmware[S8]

The crystal data, details of data collection and structure refinement parameters are summarized in Table S3. The positions of all non-hydrogen atoms were determined by direct methods using SIR-97.[S9] All non-hydrogen atoms were refined anisotropically using weighted full-matrix least-squares on F^2. Refinement and further calculations were carried out using SHELXL-97.[S10]

All hydrogen atoms bonded with carbon atoms were positioned with an idealized geometry and refined using a riding model with $U_{iso}(H)$ fixed at 1.2 U_{eq} of C. The hydrogen atoms of protonated pyridines were identified on difference Fourier maps and refined with restrained N-H distances to preserve proper geometry. Crystallographic information file (CIF) has been deposited with the Cambridge Crystallographic Data Centre (CCDC): CCDC-977338. Copy of the data can be obtained free of charge via http://www.ccdc.cam.ac.uk/conts/retrieving.html, or from the Cambridge Crystallographic Data Centre, 12 Union Road, Cambridge CB2 1EZ, UK; fax: +44 1223 336 033; or e-mail: deposit@ccdc.cam.ac.uk.

Table S3. Crystal data and structure refinement parameters for $(pyH)_3[Mn(NCS)_5]$.

empirical formula	$C_{20}H_{18}MnN_8S_5$
formula weight	585.66
crystal size (mm)	0.36x0.31x0.22
crystal system	Monoclinic
space group	*C*2/*c*
a (Å)	11.928(5)
b (Å)	13.662(5)
c (Å)	17.417(5)
α (deg)	90.000(5)
β (deg)	105.321(5)
γ (deg)	90.000(5)
V (Å^3)	2737.4(17)
Z	4
T (K)	293(2)
D_c (Mg/m^3)	1.421
μ (mm^{-1})	0.888
reflections measured	19259
reflections unique	2640
reflections observed [$I > 2\sigma(I)$]	2295
R indices [$I > 2\sigma(I)$]	
R	0.0462
wR_2	0.1226
S	1.049

Table S4. Selected bond lengths (Å) and angles (°) for $(pyH)_3[Mn(NCS)_5]$.

Bond lengths	
Mn–N	
Mn1–N13	2.098(4)
Mn1–N12	2.100(2)
Mn1–N11	2.209(3)
S–C	
S11–C11	1.618(3)
S12–C12	1.584(3)
S13–C13	1.591(4)
C–N	
C11–N11	1.154(4)
C12–N12	1.133(4)
C13–N13	1.133(5)
Bond angles	
N–Mn–N	
N13–Mn1–N12	119.84(8)
N13–Mn1–N11	90.46(7)
N12–Mn1–N12	120.32(16)
N12–Mn1–N11	89.66(11)
N11–Mn1–N11	179.09(15)
N–C–S	
N13–C13–S13	180.0
N12–C12–S12	179.4(3)
N11–C11–S11	179.6(3)
C–N–Mn	
C13–N13–Mn1	180.0
C12–N12–Mn1	177.0(3)
C11–N11–Mn1	177.0(2)

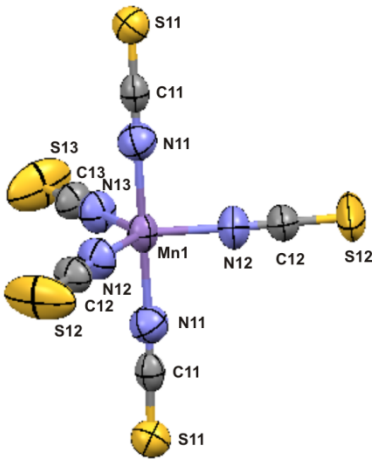

Figure S12. X-ray crystal structure of the complex anion in $(pyH)_3[Mn(NCS)_5]$ with atom labeling scheme and 50% displacement ellipsoids.

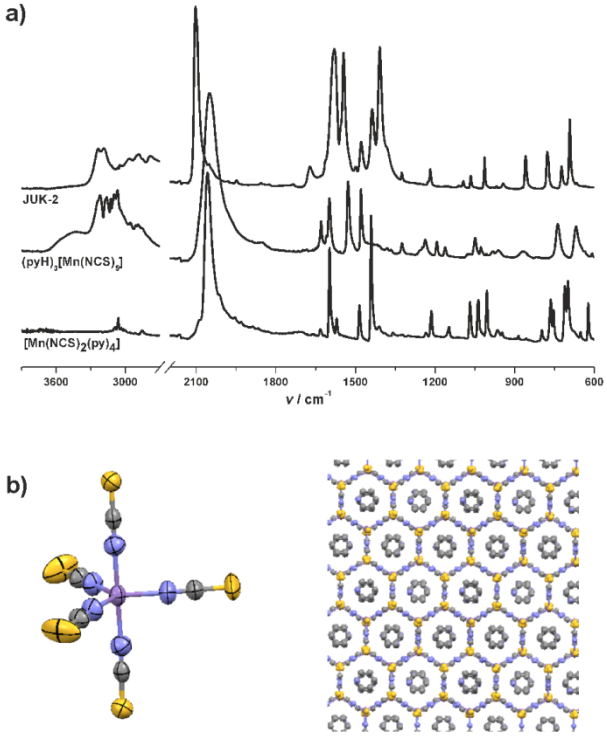

Figure S13. a) IR spectra of products of solvent-free (sf) and solvent-based (sb) reactions of JUK-1 with NH_4SCN. (top to bottom): JUK-2 (sf); $[Mn(NCS)_2(py)_4]$ (sb); $(pyH)_3[Mn(NCS)_5]$ (sb) b) Crystal structure of $(pyH)_3[Mn(NCS)_5]$: (left) the anion with thermal ellipsoids at 50% probability level (right) packing view along the [201] lattice vector. Color code: purple (Mn), blue (N), yellow (S), gray (C).

Details of other physical measurements

Carbon, hydrogen and nitrogen were determined using an Elementar Vario MICRO Cube elemental analyzer.

IR spectra were recorded on a Thermo Scientific Nicolet iS5 FT-IR spectrophotometer equipped with an iD5 diamond ATR attachment.

Electronic diffuse reflectance spectra were measured in $BaSO_4$ pellets with $BaSO_4$ as a reference using UV-3600 UV-VIS-NIR spectrophotometer equipped with ISR-260 attachment.

All powder X-ray diffraction (PXRD) patterns, except the one used for JUK-2 structure refinement (see 'PXRD data collection and structure refinement details for $\{(NH_4)_2[Mn(ina)_2(NCS)_2]\}_n \cdot xH_2O$ (JUK-2)' above), were recorded at room temperature (295K) on a Rigaku Miniflex 600 diffractometer with Cu-Kα radiation (λ = 1.5418 Å) in a 2θ range from 3° to 73° with a 0.05° step at a scan speed of 1° min^{-1}.

Thermogravimetric analyses (TGA) were performed on a Mettler-Toledo TGA/SDTA 851^e instrument, coupled with a quadrupole mass spectrometer (QMS) Thermostar GSD 300 T Balzers, at a heating rate of 10°C min^{-1} in a temperature range of 25−600 °C (sample weight approximately 20 mg). The measurement was performed at atmospheric pressure under flowing argon.

Electrical conductivity (EC) was measured using the AC quasi-four-probe method at temperature range between +5 °C and +50 °C and at a fixed low frequency of 33Hz to avoid the sample polarization, what is typical in case of the DC measurements of MIEC (Mixed Ionic Electronic Conduction) materials. A small stabilized current of 50 μA was applied during the measurements to avoid non-ohmic issue of the sample. Prior to the measurement the MOF sample was conditioned for at least 40h at desired RH conditions in a humidity chamber Memmert HCP 246. Then, powdered MOF sample was placed in a glass tube and pressed by a screw-press between parallel gold disc electrodes (ϕ=5mm) till the measured resistance remained constant, i.e. the best physical electrical contact was achieved. To assure no changes in MOF hydration during the measurement a sample chamber was completely filled by MOF powder (there was no free volume) and sealed. At the same time relatively narrow temperature range for measurement was applied. By this method temperature dependence of electrical conductivity and activation energy of electrical conductivity can be evaluated for materials showing values > 10^{-7} S cm^{-1}.

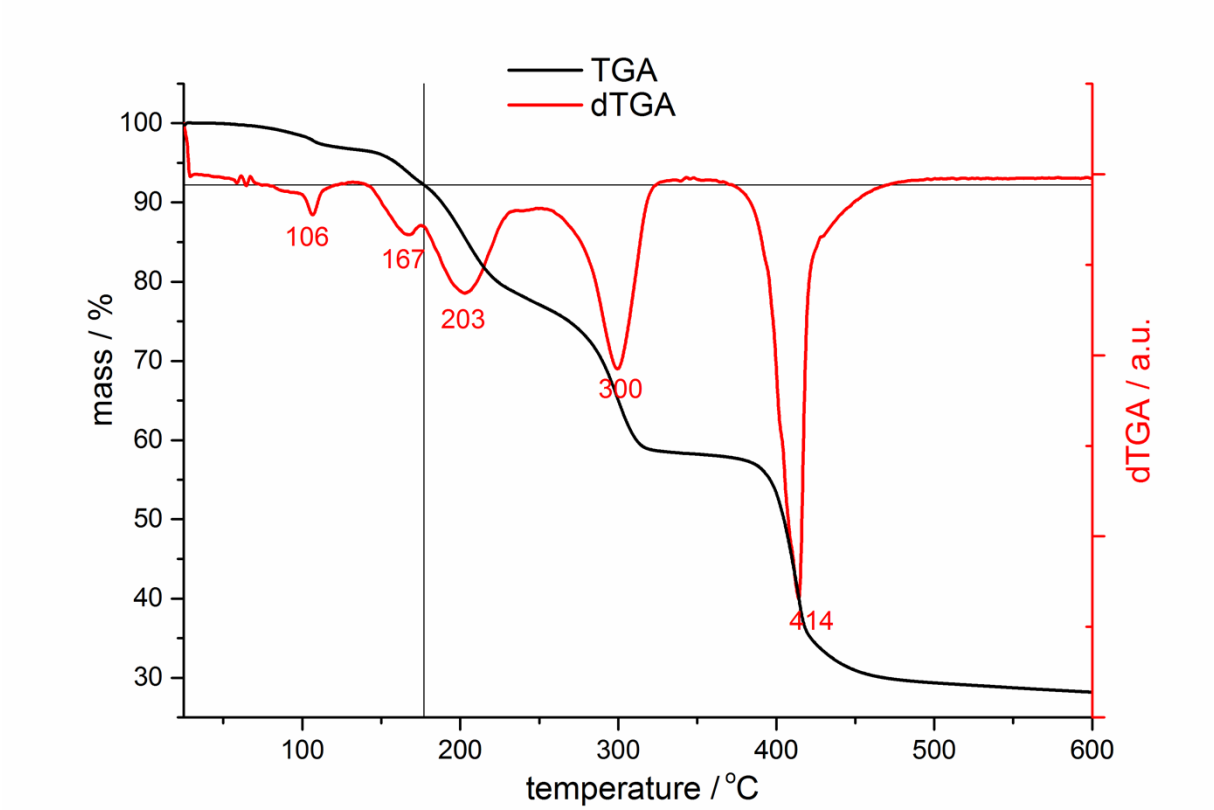

Figure S14. TGA (black) and dTGA (red) curves for $\{(NH_4)_2[Mn(ina)_2(NCS)_2]\}_n \cdot xH_2O$ (JUK-2) showing stepwise weight loss upon heating.

TGA/QMS for $\{(NH_4)_2[Mn(ina)_2(NCS)_2]\}_n \cdot xH_2O$ (JUK-2) revealed a stepwise weight loss (Fig. S6) upon heating. The first two distinct steps with maxima at 106 °C and 167 °C correspond to the loss of two ammonia molecules per formula unit (found: 7.78 %, *m/z* = 17 $[NH_3]^+$, $[OH]^+$, 16 $[NH_2]^+$; calculated (on anhydrous basis) weight-loss: 7.54 %) as well as some amount of water molecules (whose unambiguous presence in the as-synthesized JUK-2 has been confirmed by conductivity measurements). The subsequent three distinct steps occurring at 203, 300 and 414 °C are associated with a loss of thiocyanates, carboxylate groups and are associated with a decomposition of the compound (*m/z* = 76 $[CS_2]^+$, 59 $[HNCS]^+$, 34 $[H_2S]^+$, 44 $[COO]^+$).

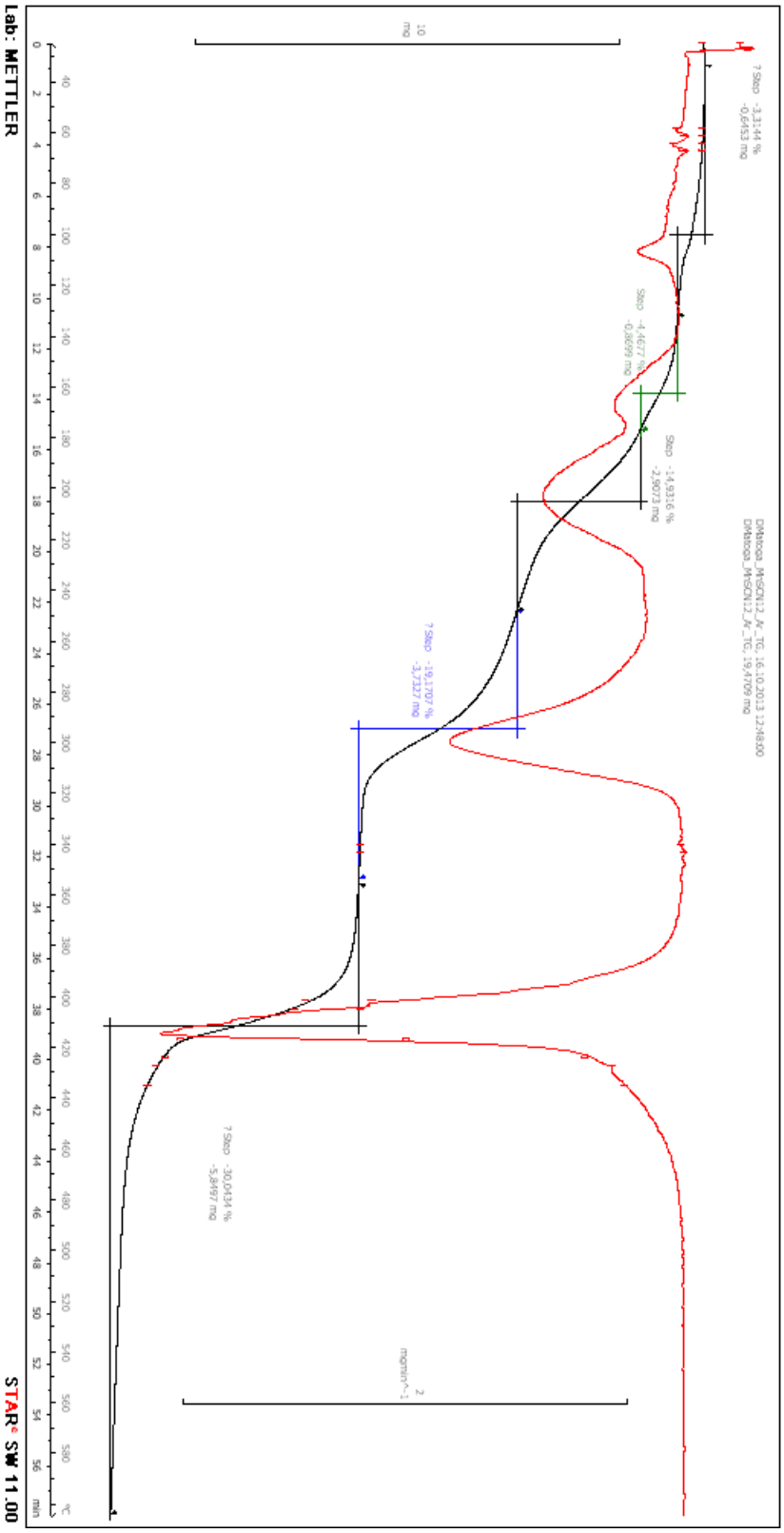

Figure S15. TGA (black) and dTGA (red) curves for $\{(NH_4)_2[Mn(ina)_2(NCS)_2]\}_n \cdot xH_2O$ (JUK-2) showing stepwise weight loss upon heating (original instrument print-out).

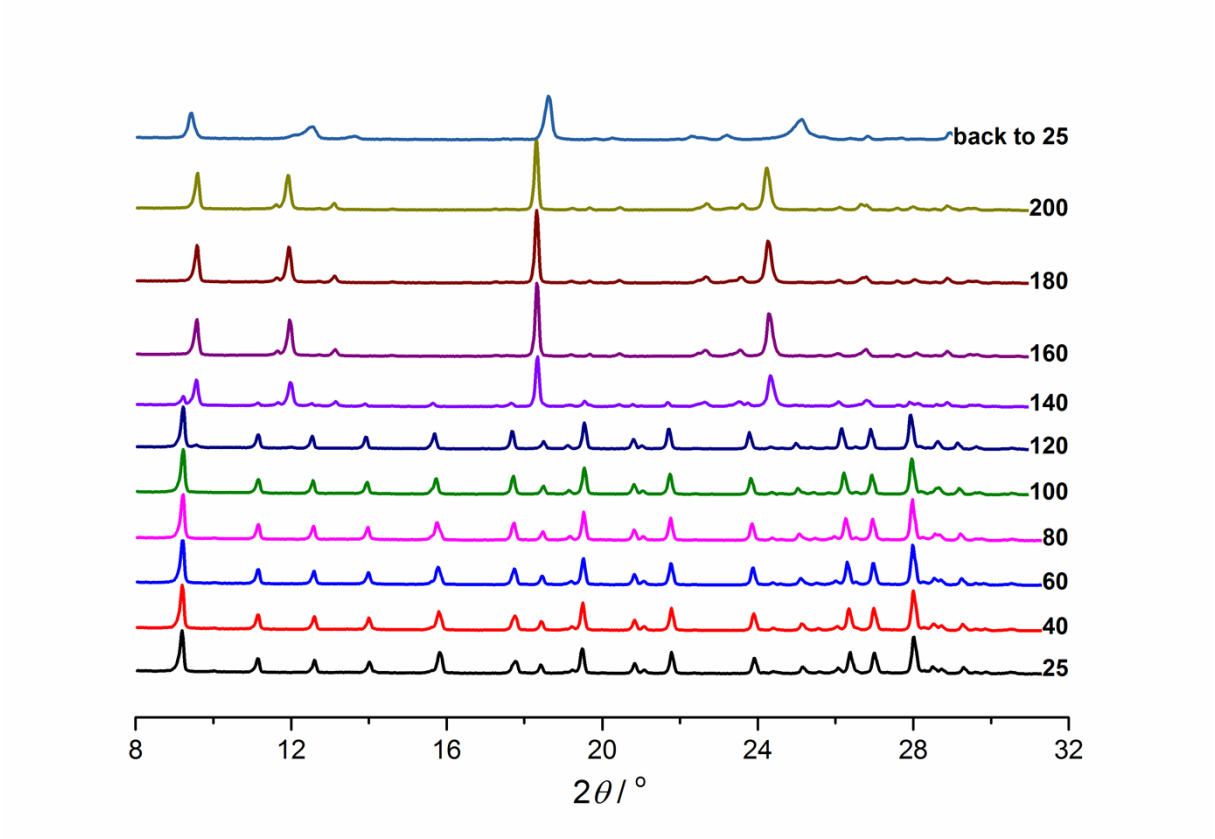

Figure S16. Temperature-dependent PXRD patterns for $(NH_4)_2[Mn(ina)_2(NCS)_2]\}_n \cdot xH_2O$ (JUK-2) . Numbers indicate temperatures in °C.

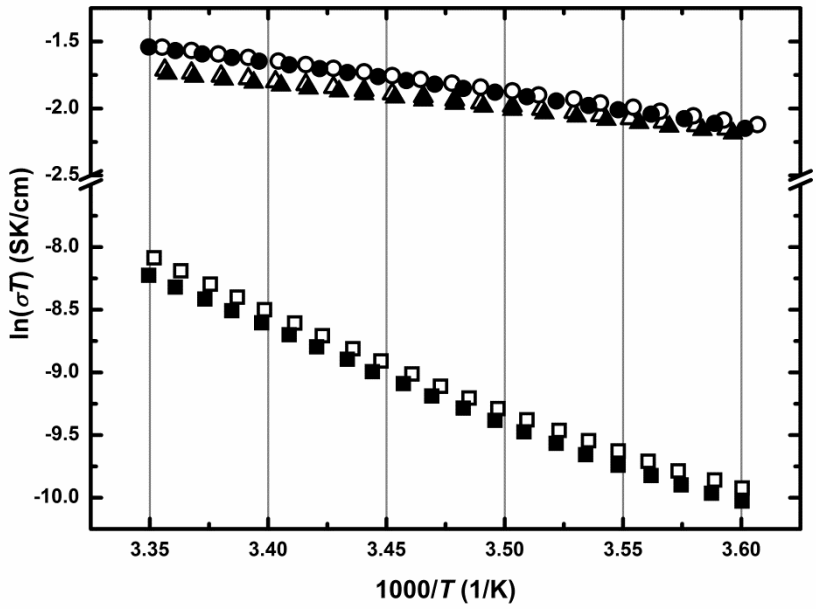

Figure S17. Proton conduction in JUK-2 PCMOF a) Arrhenius plots for a (1)→(2)→(3) sequence: (1) as-synthesized (circles); (2) dried for 3h at 60oC, 25mbar and kept in air at ambient conditions for 4 days (squares); (3) kept over water in a closed vial for 16h at 40oC and kept in air at ambient conditions for 4 days (triangles). Open and closed symbols denote cooling and heating cycles, respectively.

Comment: To verify the reversibility of conduction property, the sample of JUK-2 was dried and then stepwise humidified. It has been observed that the dried sample (3h at 60°C, 25mbar) was not conductive ($S < 10^{-7}$ S cm^{-1}). On the other hand, when the dried sample was conditioned in air at ambient conditions, only a partial restoration (1.2×10^{-6} S cm^{-1} at 25 °C) of conductivity was observed (Fig. S17). In contrast, when this sample was further exposed to 100% RH followed by conditioning at ambient conditions, the restoration of conductivity (6.3×10^{-4} S cm^{-1} at 25°C) was observed.

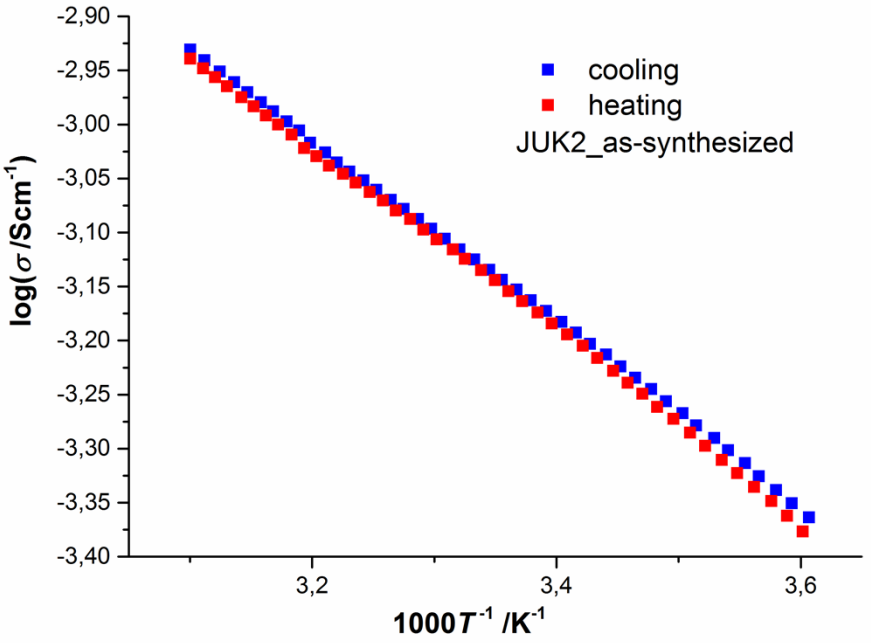

Figure S18. Proton conduction reversibility in JUK-2 (as-synthesized) within 5-50°C range. First cycle is cooling (blue symbols) followed by a heating cycle (red symbols).

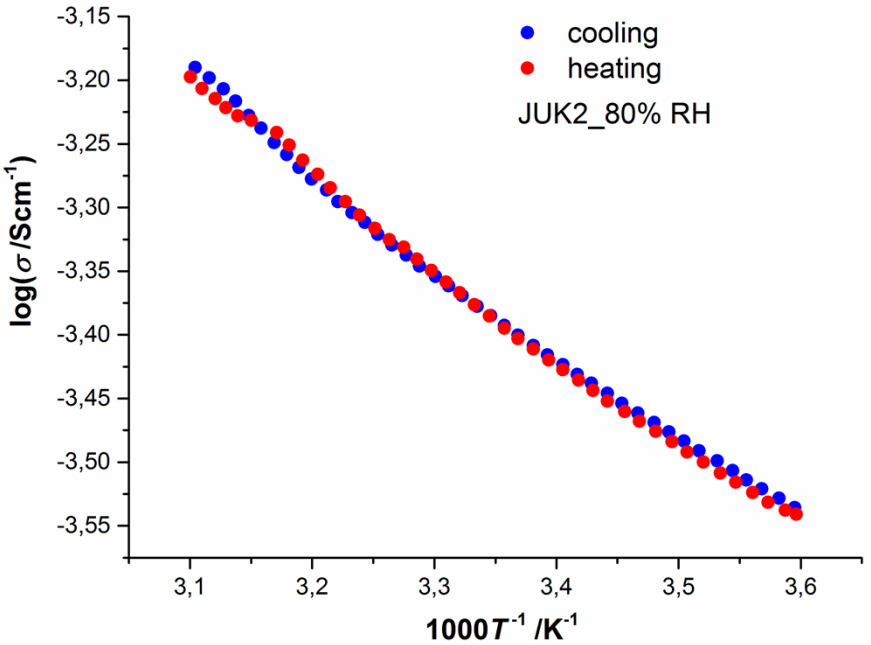

Figure S19. Proton conduction reversibility in JUK-2 (conditioned at 80% RH, 35°C**) within 5-50°C range. First cycle is cooling (blue symbols) followed by a heating cycle (red symbols).**

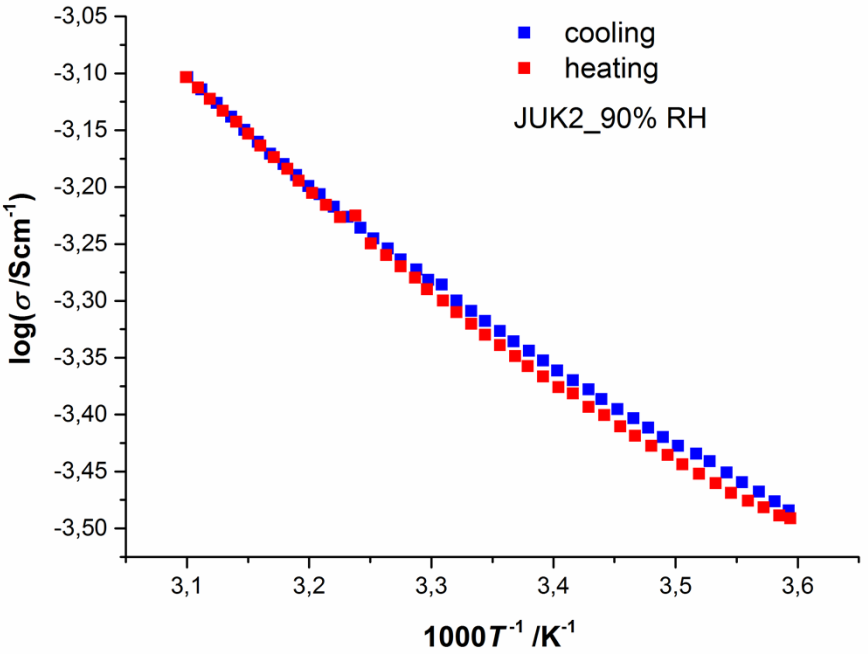

Figure S20. Proton conduction reversibility in JUK-2 (conditioned at 90% RH, 35°C**) within 5-50°C range. First cycle is cooling (blue symbols) followed by a heating cycle (red symbols).**

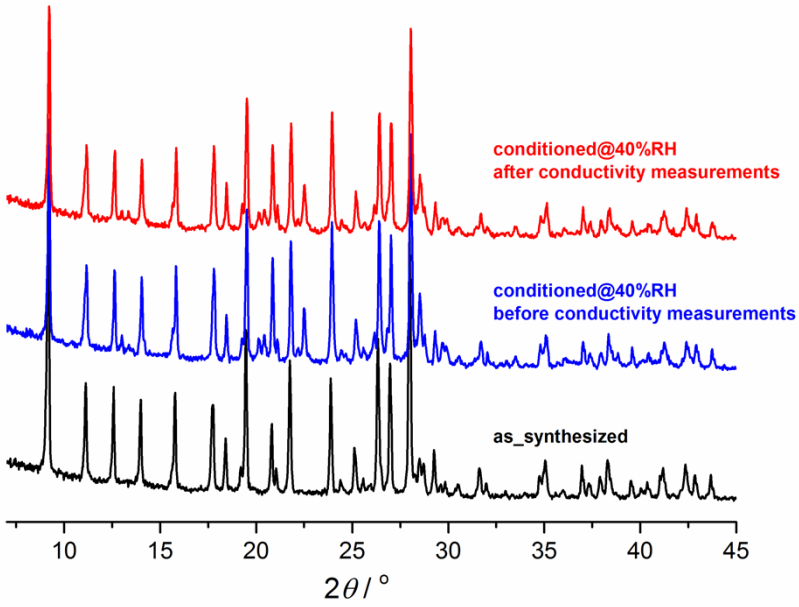

Figure S21. PXRD patterns for $(NH_4)_2[Mn(ina)_2(NCS)_2]\}_n \cdot xH_2O$ (JUK-2) conditioned at 40% RH at 35°C: before and after proton conductivity measurements. PXRD pattern of the as-synthesized JUK-2 is given for comparison.

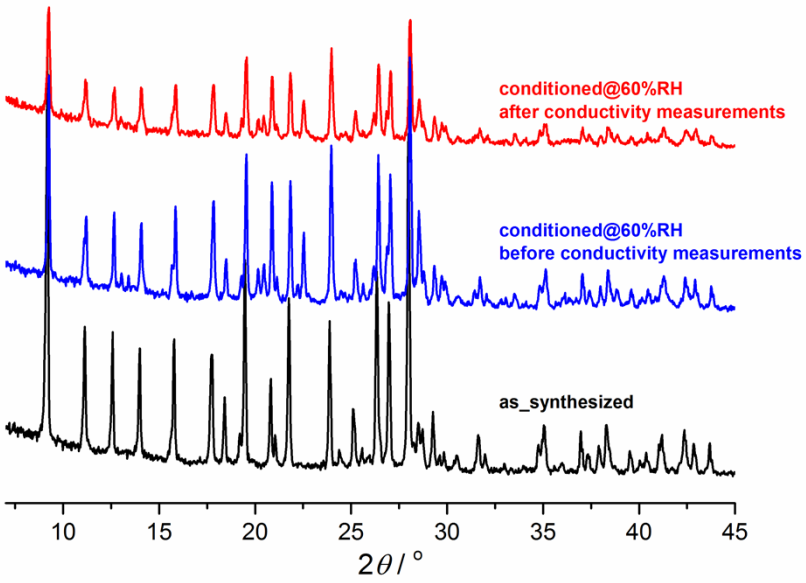

Figure S22. PXRD patterns for $(NH_4)_2[Mn(ina)_2(NCS)_2]\}_n \cdot xH_2O$ (JUK-2) conditioned at 60% RH at 35°C: before and after proton conductivity measurements. PXRD pattern of the as-synthesized JUK-2 is given for comparison.

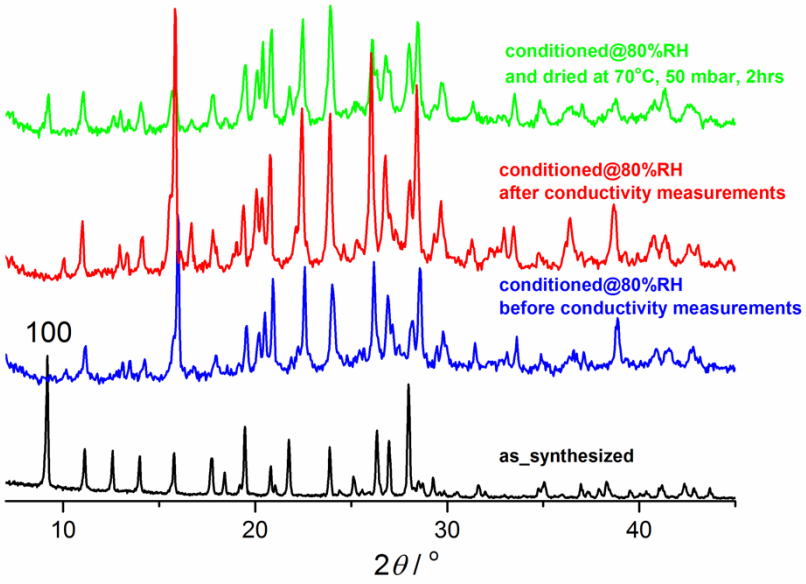

Figure S23. PXRD patterns for $(NH_4)_2[Mn(ina)_2(NCS)_2]\}_n \cdot xH_2O$ (JUK-2) conditioned at 80% RH at 35°C: before and after proton conductivity measurements. PXRD pattern of the as-synthesized JUK-2 (red curve) and the sample dried after conditioning (green curve), are given for comparison.

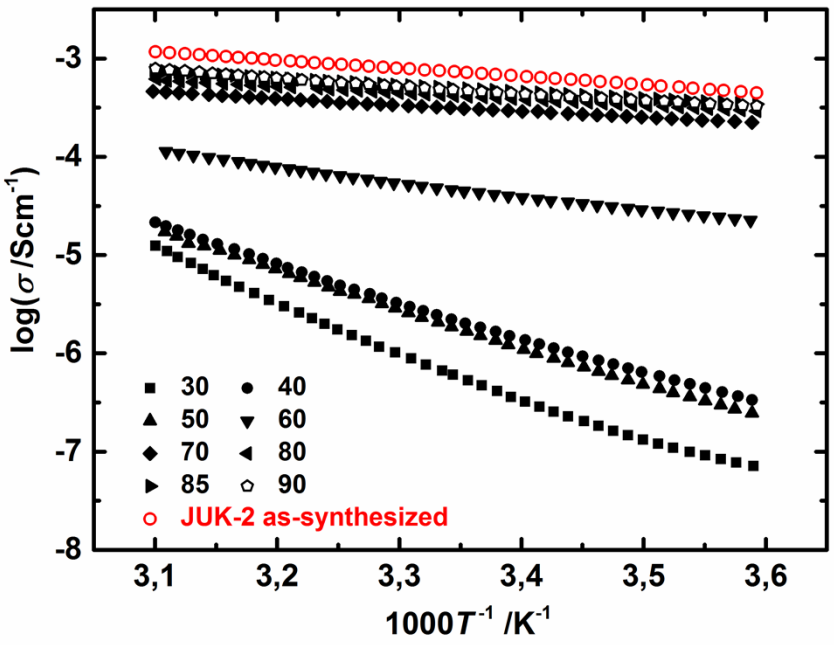

Figure S24. Proton conductivity in JUK-2 PCMOF for various values of relative humidity (indicated by numbers).

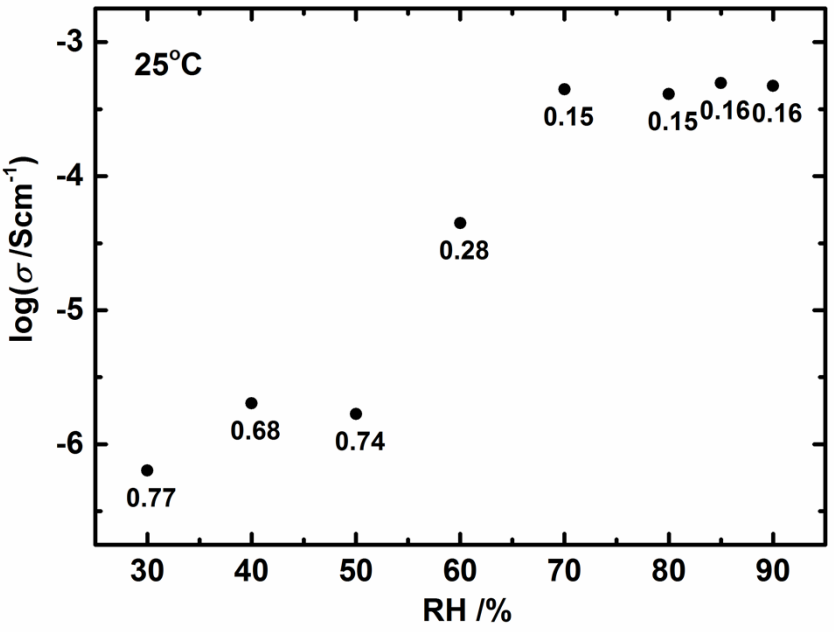

Figure S25. Proton conductivity *vs* relative humidity (RH) for JUK-2 PCMOF at 25°C. Numbers indicate activation energy for proton conduction.

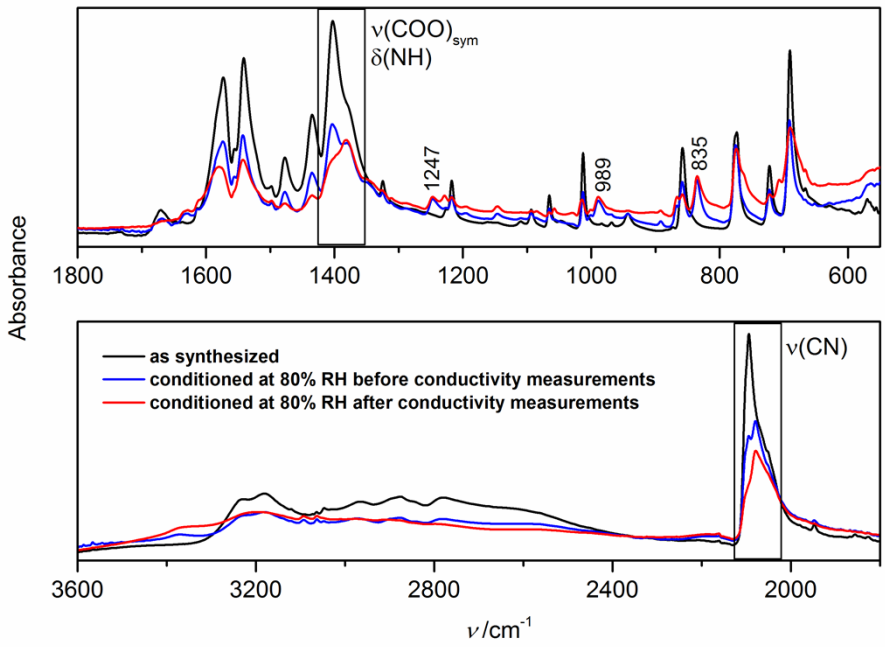

Figure S26. IR spectra for $(NH_4)_2[Mn(ina)_2(NCS)_2]\}_n \cdot xH_2O$ (JUK-2) conditioned at 80% RH at 35°C: before and after proton conductivity measurements. IR spectrum of the as-synthesized JUK-2 is given for comparison.

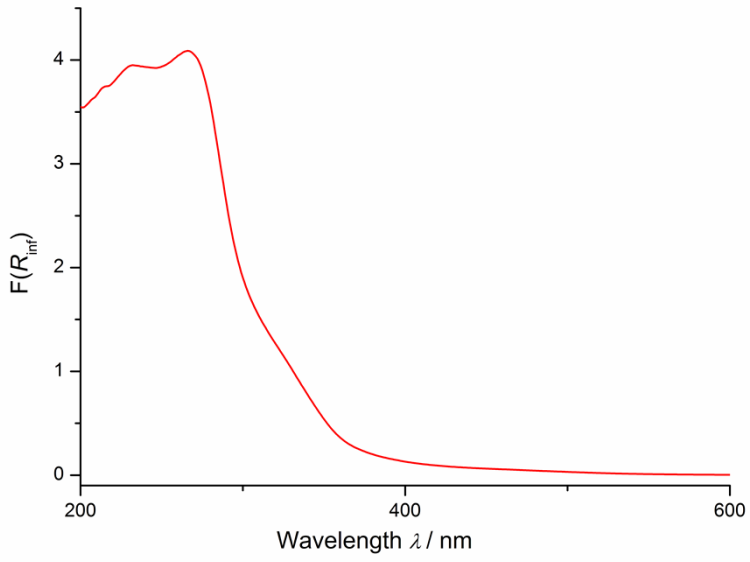

Figure S27. UV-vis diffuse reflectance spectra (after Kubelka-Munk transformation) of $\{(NH_4)_2[Mn(ina)_2(NCS)_2]\}_n \cdot xH_2O$ (JUK-2).

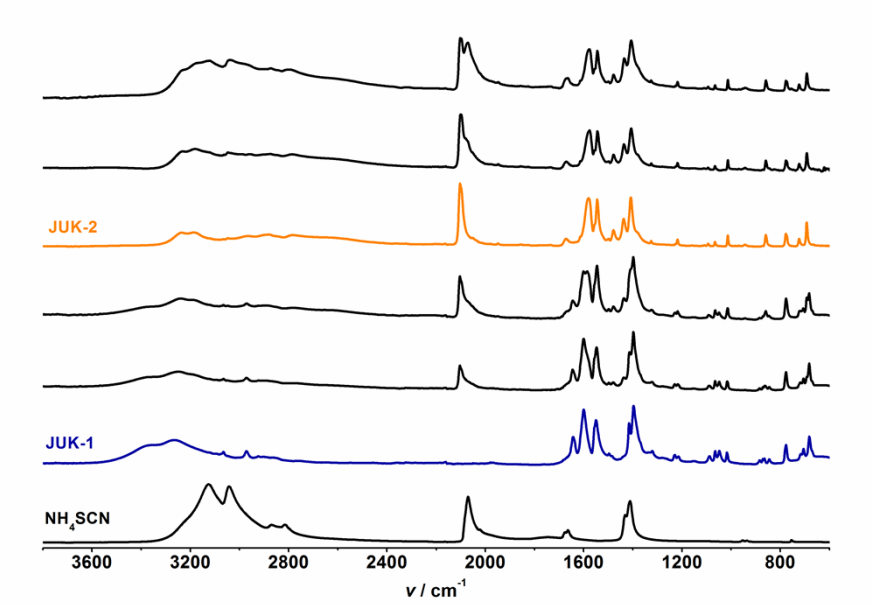

Figure S28. JUK-2 formation upon 5 min LAG (EtOH) grinding of JUK-1 and NH_4SCN at various stoichiometries (given as JUK-1 to NH_4SCN ratio). a) IR-ATR spectra of ground reactants (top to bottom): 1:3.5; 1:2.7; 1:2 (pure JUK-2); 1:1; 1:0.5; initial JUK-1; initial NH_4SCN.

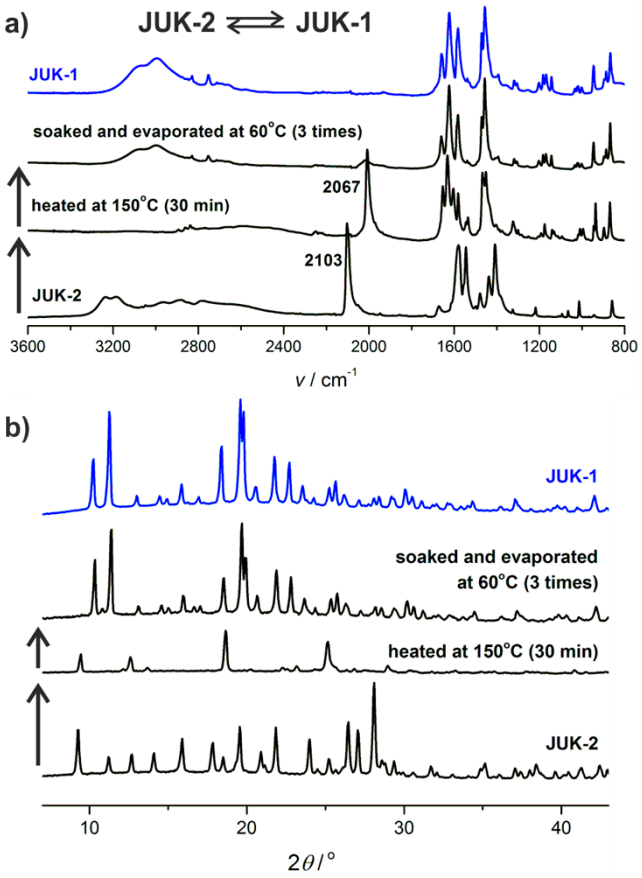

Figure S29. Reversibility of JUK-2 formation. IR spectra (a) and PXRD patterns (b): (bottom to top) initial JUK-2; JUK-2 heated; JUK-2 heated, soaked in EtOH and evaporated (with stirring); JUK-1 (blue line).

Table S5. Key structural features and performance indicators for proton conducting JUK-2 (as-synthesized and humidified)

Sample	**Structural features (PXRD)**	**Relative humidity RH (%RH)**	**Conductivity σ (S/cm) at 25 °C**	**Activation energy E_a (eV)**	**Key ions/molecules forming conduction pathway (major location)**	**Proposed mechanism**
as-synthesized (contact with 92% ethanol)	pure JUK-2 phase crystal structure does not include water molecules	kept under ambient conditions in air (~20-22°C)	7.2×10^{-4}	0.16	NH_4^+ (interlayer) H_2O (disordered, interlayer space saturated with water) dried JUK-2 not conductive; JUK-2 with thermally removed ammonia not conductive (even when humidified at 80%RH)	Grotthuss mechanism prevails through interlayer space
humidified (RH ≤ 60%) at 35°C for at least 40h	JUK-2 phase + minor amount of a new phase that appears as a result of equilibrium between pure JUK-2 phase and water new five weak signals in the PXRD pattern (attributed to the new phase); bulk interlayer separation in JUK-2 intact	≤ 60%	$\sigma < 4\times10^{-6}$ (RH = 30-50%) $\sigma = 4.5\times10^{-5}$ (RH = 60%)	$E_a = 0.73$ (average for RH = 30-50%) $E_a = 0.28$ (RH = 60%)	NH_4^+ (interlayer) H_3O^+ (minor amount, interlayer) H_2O (interlayer)	vehicular mechanism prevails through interlayer space
humidified (RH ≥ 70%) at 35°C for at least 40h	JUK-2 phase + a new phase (the same as for samples at RH≤ 60%)	≥ 70%	$\sigma \approx$ const. $\sigma = 4.6\times10^{-4}$ (average)	$E_a \approx$ const. $E_a = 0.15$ (average)	NH_4^+ (surface of exfoliated layers and intergrain) H_3O^+ (surface of exfoliated layers and intergrain)	Grotthuss mechanism prevails on the surface of

	the five PXRD signals of the new phase more pronounced; bulk interlayer separation in JUK-2 removed (the 100 reflection disappears and reappears after drying)		'saturation' effect		H_2O (surface of exfoliated layers and intergrain) water enters bulk interlayer region, layers exfoliated, condensed water on the surface of hygroscopic sample	exfoliated layers and through intergrain space

References in the Supporting Information:

S1. D. Matoga, B. Gil, W. Nitek, A. D. Todd, C. W. Bielawski, *CrystEngComm*, 2014, **16**, 4959.

S2. J. G. Małecki, B. Machura, A. Świtlicka, T. Groń, M. Bałanda, *Polyhedron*, 2011, **30**, 746.

S3. A. Altomare, G. Campi, C. Cuocci, L. Eriksson, C. Giacovazzo, A. Moliterni, R. Rizzi, P.-E. Werner, *J. Appl. Cryst.*, 2009, **42**, 768.
Advances in powder diffraction pattern indexing: N-TREOR09.

S4. A. Altomare, C. Cuocci, C. Giacovazzo, A. Moliterni, R. Rizzi, N. Corriero, A. Falcicchio, *J. Appl. Cryst.*, 2013, **46**, 1231.
EXPO2013: a kit of tools for phasing crystal structures from powder data.

S5. V. Favre-Nicolin, R. Cerny, *J. Appl. Cryst.*, 2002, **35**, 734.
FOX, 'free objects for crystallography': a modular approach to ab initio structure determination from powder diffraction.

S6. V. Petricek, M. Dusek, L. Palatinus, 2006, *Jana2006. The crystallographic computing system. Institute of Physics, Praha, Czech Republic.*

S7. H. M. Rietveld, *J. Appl. Crystallogr.*, 1969, **2**, 65.
A profile refinement method for nuclear and magnetic structures.

S8. Oxford Diffraction (2010). CrysAlis PRO. Oxford Diffraction Ltd, Yarnton, England.

S9. A. Altomare, M. C. Burla, M. Camalli, G. L. Cascarano, C. Giacovazzo, A. Guagliardi, A. G. G. Moliterni, G. Polidori, R. Spagna, *J. Appl. Cryst.*, 1999, **32**, 115.

S10. G. M. Sheldrick, *Acta Cryst.* 2008, **A64**, 112.